

Seismic Properties of Samples from the Volcanic Section of the Troodos Ophiolite, Hole CY-2a

NIKOLAS I. CHRISTENSEN¹, WILLIAM W. WEPFER¹ AND MATTHEW H. SALISBURY²

¹Department of Earth and Atmospheric Sciences, Purdue University,
West Lafayette, Indiana, U.S.A.

²Centre for Marine Geology, Dalhousie University, Halifax, Nova Scotia, Canada

Christensen, N.I., Wepfer, W.W. and Salisbury, M.H., Seismic properties of samples from the volcanic section of the Troodos Ophiolite, Hole CY-2a; in Cyprus Crustal Study Project: Initial Report, Holes CY-2 and 2a, ed. P.T. Robinson, I.L. Gibson and A. Panayiotou; Geological Survey of Canada, Paper 85-29, p. 307-315, 1987.

Abstract

Compressional and shear wave velocities are reported to confining pressures of 600 MPa for 17 altered igneous samples from ICRDG Hole CY-2a in the Troodos Ophiolite. Velocities increase with increasing depth and correlate well with bulk density and porosity. The compressional wave velocity gradient (dV_p/dZ) is approximately 2.1/s in good agreement with a Layer 2 velocity gradient of 1.9/s reported in the Pacific at DSDP Site 504B by Stephen and Harding (1983). Since pillow basalts are uncommon in the section and the intensity and grade of metamorphism increase with depth, our results suggest that positive velocity gradients similar to those observed in oceanic Layer 2 can be produced by changes in microporosity and metamorphic grade.

Résumé

Les vitesses des ondes de compression et de cisaillement à des pressions de confinement de 600 MPa ont été déterminées pour 17 échantillons de roches ignées altérées du trou de forage CY-2a, ICRDG, dans l'ophiolite de Troodos. Les vitesses augmentent avec l'accroissement de la profondeur et la corrélation est excellente avec la densité apparente et la porosité. Le gradient de la vitesse des ondes de compressions (dV_p/dZ) est approximativement 2,1/s, en accord le gradient de vitesse de 1,9/s pour la Couche 2 dans le Pacifique obtenu au site 504B du projet DSDP par Stephen et Harding (1983). Vu que les basaltes en coussinets sont peu abondants dans la section et que l'intensité et le degré du métamorphisme croissent avec la profondeur, nos résultats révèlent que les gradients de vitesse positifs similaires à ceux observés dans la Couche 2 océanique peuvent être dus à des changements de microporosité et de degré de métamorphisme.

INTRODUCTION

During the past two decades our knowledge of Layer 2 of the oceanic crust has increased considerably. While early oceanic seismic refraction studies (e.g. Raitt, 1963) only provided average compressional wave velocities for Layer 2, more detailed sonobuoy techniques enabled Houtz and Ewing (1976) to subdivide Layer 2 into three units: an upper unit (2A) with velocities below 4 km/s, an intermediate unit (2B) with velocities between 4.8 and 5.7 km/s, and a lower unit (2C) with velocities in excess of 6.0 km/s. More recent studies using amplitude as well as travel time analysis have shown that the velocity structure of Layer 2 consists of gradients (Helmberger and Morris, 1969) and velocity logs obtained to a sub-basement depth of 1030 m in DSDP Hole 504B substantiate these models (Salisbury et al., 1985). Upper Layer 2 compressional wave velocities corresponding to Layer 2A are 4.0 km/s or less. Velocities generally increase with depth to 1 km, where they reach 6.0 km/s.

Worldwide recovery by DSDP of samples from the basement demonstrates that basalt is the most common rock type forming the upper portion of Layer 2. Since laboratory measurements of velocities in DSDP basaltic rocks at appropriate confining pressures and conditions of water saturation are generally much higher than 4.0 km/s (Christensen and Salisbury, 1975), it is generally concluded that the velocities in Layer 2A are lowered by the presence of porosity in the form of large scale fractures and rubble zones (Hyndman and Drury, 1976) and that the observed gradients reflect decreasing crack porosity with depth. Compressional wave velocities in basalt samples collected from the Bay of Islands and Samail ophiolites are also higher than the Layer 2 velocities determined by seismic refraction and logging (Salisbury and Christensen, 1978; Christensen and Smewing, 1981), supporting the crack porosity model.

Between 1983 and 1985, the International Crustal Research Drilling Group (ICRDG) drilled an array of holes through different stratigraphic levels of the Troodos Ophiolite in an attempt to reconstruct the petrology, geochemistry and geophysical properties of the complex as a function of depth for comparison with the results of drilling and geophysical studies at sea. While many of the results are consistent with those observed at sea (the volcanic section grades downward from pillow basalts at the sediment/basement contact through sheeted dykes at depth and the metamorphic grade increases markedly with depth), some features are quite different (the volcanic section is composed of andesites and basaltic andesites rather than tholeiites and contains a high proportion of massive sheet flows), leading the ICRDG investigators to characterize the complex as

oceanic with island arc affinities.

In this paper, we present laboratory velocity data for 17 samples obtained from various depths in Hole CY-2a which was spudded near the village of Agrokipia in the vicinity of the pillow basalt/sheet flow transition about 200 m below the sediment/basement contact and penetrated a mineralized stockwork zone. As can be seen in Table 1, the hole was drilled through a 689 m section of dykes, sills, sheet flows and minor pillows of predominantly andesitic composition. Importantly, the core shows a marked increase in the intensity and grade of metamorphic alteration with depth: from 0-149 m (Units I-VI), the section shows evidence of variable low temperature alteration (halmyrolysis); glass is locally preserved but is often partially replaced, along with the groundmass, by smectite and minor calcite. From 149-297 m (Units VII-X), the section has undergone pervasive hydrothermal alteration: the rocks are cream-coloured, pyrite is abundant (up to 10%), and the groundmass has been almost completely replaced by chlorite and illite plus minor calcite, quartz and zeolites. Between 297-689 m, the section has undergone pervasive greenschist facies alteration, with the groundmass being completely replaced by chlorite, epidote, quartz and albite plus minor calcite and pyrite. Although the section drilled cannot be regarded as strictly equivalent to oceanic Layer 2, the data from this interval suggests an alternate origin for velocity gradients such as those observed in Layer 2.

EXPERIMENTAL TECHNIQUE AND DATA

Compressional and shear wave velocity measurements were made on the samples at elevated pressures using the pulse transmission method summarized by Birch (1960) and described in detail by Christensen (1985). Minicores were taken perpendicular to the drill core (i.e. horizontal relative to the surface) using a diamond drill. The ends of the samples were then cut with a diamond cut-off saw to form a right circular cylinder and hand polished on a lap wheel until flat and parallel to within 0.008 cm. Typical dimensions for the samples after cutting and polishing were 2.54 cm in diameter and 4.00 cm in length. After the dry bulk densities had been determined from the mass and dimensions of each sample, the cores were saturated by placing them in distilled water and pulling a moderate vacuum. The wet bulk densities and effective porosities presented in Table 2 were then determined by re-weighing the samples.

Each sample was surrounded with a fine mesh copper screen and jacketed in copper foil. The screen allowed for the migration of fluid from the pores while the sample was under pressure to prevent

excessive pore pressure build up. Brass shim discs were spot soldered on each end of the copper jackets to provide an electrical ground for the transducers.

Appropriately oriented lead zirconate titanate (PZT) transducers of nominal 1 MHz resonant frequency were used both in the compressional measurements and as the receiving transducers in the shear wave velocity determinations. AC cut quartz crystals were the sending transducers for the shear wave measurements. Each transducer was mounted on a brass electrode through which the electrical connection was made. A transducer was placed on each end of the core in contact with the brass shim

disc and gum rubber tubing was fitted over the interface to exclude the pressure medium.

The sample assembly was then placed in the hydraulic press described by Christensen (1985) and velocities were measured to 600 MPa (6 kbar) using a calibrated mercury delay line. The values obtained, together with bulk modulus (K), shear modulus (μ), Poisson's ratio (σ) and V_p/V_s values calculated from the velocities and densities at selected pressures, are given in Table 2. The velocities and densities used in the calculations were corrected for length and volume changes at elevated pressures using an iterative routine and dynamically determined compressibilities.

TABLE 1. Lithology, Petrology and Nature of Alteration vs. Depth in Hole CY-2a*

Depth (m)	Unit	Lithology	Petrology	Alteration
3.35-30.72	I	Dikes/Sills	Basaltic Andesite	
31.15-67.50	III	Sheet Flows	Andesite and Basaltic Andesite	Variable, low temperature alteration. Groundmass fresh to strongly replaced by dark green clay plus minor calcite, zeolites.
67.50-89.90	IV	Dikes/Sills	Basaltic Andesite	
89.90-109.00	V	Sheet Flows	Andesite	
109.00-297.14	VI-X	Glassy Sheet Flows	Andesite	Variable, low temperature alteration to smectite; glass locally preserved. Pervasive hydrothermal alteration. Groundmass replaced by chlorite, illite, plus minor calcite, smectite, quartz, celadonite. Pyrite abundant.
297.49-403.80	XII-XIV	Dikes/Sills	Andesites	
403.80-528.90	XV-XXI	Pillows/Screens	Andesite & Dacite	Pervasive high temperature alteration. Groundmass replaced by chlorite, epidote, quartz, albite.
528.90-689.15	XXII	Dikes/Sills	Andesite	

*(after Robinson and Gibson, 1983; Bednarz et al., 1987)

TABLE 2. Compressional (V_p) and Shear (V_s) Wave Velocities, Densities (ρ), Porosities (ϕ), Poisson's Ratios (σ), Bulk Moduli (K), and Shear Moduli (μ) of CY-2a Rocks

Sample Depth	P (MPa)	V_p (km/s)	V_s (km/s)	V_p/V_s	σ	K (MPa $\times 10^5$)	μ (MPa $\times 10^5$)
10.25 m $\rho = 2.37 \text{ g cm}^{-3}$ $\phi = 16.8\%$	20	3.39	2.05	1.65	0.21	0.14	0.10
	40	3.43	2.08	1.65	0.21	0.14	0.10
	60	3.48	2.11	1.65	0.21	0.15	0.11
	80	3.53	2.18	1.62	0.19	0.15	0.11
	100	3.59	2.20	1.63	0.20	0.15	0.12
	200	3.83	2.27	1.69	0.23	0.19	0.12
	400	4.25	2.37	1.79	0.27	0.25	0.13
84.31 m $\rho = 2.57 \text{ g cm}^{-3}$ $\phi = 6.2\%$	600	4.44	2.42	1.83	0.29	0.28	0.14
	20	4.22	2.34	1.80	0.28	0.27	0.14
	40	4.32	2.37	1.82	0.28	0.29	0.14
	60	4.34	2.39	1.82	0.28	0.29	0.15
	80	4.39	2.40	1.83	0.29	0.30	0.15
	100	4.42	2.41	1.83	0.29	0.30	0.15
	200	4.54	2.46	1.85	0.29	0.32	0.16
138.35 m $\rho = 2.46 \text{ g cm}^{-3}$ $\phi = 8.9\%$	400	4.67	2.48	1.88	0.30	0.35	0.16
	600	4.74	2.50	1.90	0.31	0.37	0.16
	20	4.30	2.39	1.80	0.28	0.27	0.14
	40	4.33	2.44	1.77	0.27	0.27	0.15
	60	4.35	2.48	1.75	0.26	0.26	0.15
	80	4.36	2.50	1.74	0.26	0.26	0.15
	100	4.37	2.52	1.73	0.25	0.26	0.16
217.90 m $\rho = 2.41 \text{ g cm}^{-3}$ $\phi = 14.0\%$	200	4.41	2.58	1.71	0.24	0.26	0.16
	400	4.48	2.62	1.71	0.24	0.27	0.17
	600	4.54	2.64	1.72	0.24	0.28	0.17
	20	3.93	2.00	1.97	0.33	0.25	0.10
	40	3.97	2.06	1.93	0.32	0.24	0.10
	60	3.99	2.10	1.91	0.31	0.24	0.11
	80	4.02	2.13	1.89	0.31	0.24	0.11
258.83 m $\rho = 2.36 \text{ g cm}^{-3}$ $\phi = 12.9\%$	100	4.03	2.15	1.88	0.30	0.25	0.11
	200	4.11	2.22	1.85	0.29	0.25	0.12
	400	4.24	2.28	1.86	0.30	0.27	0.13
	600	4.43	2.32	1.91	0.31	0.30	0.13
	20	3.93	2.02	1.94	0.32	0.24	0.10
	40	3.96	2.06	1.92	0.31	0.24	0.10
	60	3.99	2.10	1.90	0.31	0.24	0.10

Sample Depth	P (MPa)	V _p (km/s)	V _s (km/s)	V _p /V _s	σ	K (MPa x 10 ⁵)	μ (MPa x 10 ⁵)
260.28 m $\rho = 2.49 \text{ g cm}^{-3}$ $\phi = 10.2\%$	20	4.53	2.30	1.97	0.33	0.34	0.13
	40	4.55	2.36	1.93	0.32	0.33	0.14
	60	4.57	2.39	1.91	0.31	0.33	0.14
	80	4.59	2.42	1.90	0.31	0.33	0.15
	100	4.60	2.44	1.89	0.30	0.33	0.15
	200	4.67	2.51	1.86	0.30	0.33	0.16
	400	4.78	2.58	1.85	0.30	0.35	0.17
278.59 m $\rho = 2.37 \text{ g cm}^{-3}$ $\phi = 12.8\%$	600	4.89	2.64	1.85	0.29	0.37	0.17
	20	3.88	2.07	1.87	0.30	0.22	0.10
	40	3.92	2.13	1.84	0.29	0.22	0.11
	60	3.95	2.15	1.84	0.29	0.22	0.11
	80	3.98	2.17	1.83	0.29	0.23	0.11
	100	4.01	2.19	1.83	0.29	0.23	0.11
	200	4.12	2.28	1.81	0.28	0.24	0.12
320.01 m $\rho = 2.55 \text{ g cm}^{-3}$ $\phi = 5.2\%$	400	4.30	2.40	1.79	0.27	0.26	0.14
	600	4.46	2.49	1.79	0.27	0.28	0.15
	20	4.48	2.46	1.82	0.28	0.31	0.15
	40	4.51	2.50	1.81	0.28	0.31	0.16
	60	4.53	2.53	1.79	0.27	0.31	0.16
	80	4.51	2.56	1.76	0.26	0.30	0.17
	100	4.57	2.58	1.77	0.27	0.31	0.17
364.31 m $\rho = 2.59 \text{ g cm}^{-3}$ $\phi = 3.9\%$	200	4.63	2.66	1.74	0.25	0.31	0.18
	400	4.69	2.72	1.72	0.25	0.31	0.19
	20	4.70	2.61	1.80	0.28	0.34	0.18
	40	4.72	2.64	1.79	0.27	0.34	0.18
	60	4.74	2.66	1.78	0.27	0.34	0.18
	80	4.76	2.75	1.73	0.25	0.33	0.20
	100	4.80	2.70	1.78	0.27	0.34	0.19
385.01 m $\rho = 2.54 \text{ g cm}^{-3}$ $\phi = 4.5\%$	200	4.88	2.76	1.77	0.26	0.35	0.20
	400	4.98	2.83	1.76	0.26	0.37	0.21
	20	4.75	2.65	1.80	0.28	0.34	0.18
	40	4.78	2.67	1.79	0.27	0.34	0.18
	60	4.80	2.69	1.78	0.27	0.34	0.18
	80	4.82	2.71	1.78	0.27	0.34	0.19
	100	4.83	2.72	1.77	0.27	0.34	0.19
402.50 m $\rho = 2.58 \text{ g cm}^{-3}$ $\phi = 6.8\%$	200	4.87	2.77	1.76	0.26	0.34	0.20
	400	4.94	2.83	1.75	0.26	0.35	0.20
	20	4.64	2.45	1.89	0.31	0.35	0.16
	40	4.68	2.53	1.85	0.29	0.35	0.16
	60	4.71	2.58	1.83	0.29	0.35	0.17
	80	4.73	2.61	1.81	0.28	0.34	0.18
	100	4.75	2.64	1.80	0.28	0.34	0.18
200	4.81	2.73	1.76	0.26	0.34	0.19	
	400	4.92	2.83	1.74	0.25	0.35	0.21

Sample Depth	P (MPa)	V _p (km/s)	V _s (km/s)	V _p /V _s	σ	K (MPa x 10 ⁵)	μ (MPa x 10 ⁵)
426.35 m $\rho = 2.48 \text{ g cm}^{-3}$ $\phi = 15.2\%$	20	4.20	2.39	1.76	0.26	0.25	0.14
	40	4.22	2.42	1.75	0.26	0.25	0.14
	60	4.24	2.43	1.75	0.26	0.25	0.15
	80	4.26	2.45	1.74	0.25	0.25	0.15
	100	4.27	2.45	1.74	0.25	0.25	0.15
	200	4.34	2.48	1.75	0.26	0.26	0.15
	400	4.45	2.50	1.78	0.27	0.29	0.16
476.30 m $\rho = 2.50 \text{ g cm}^{-3}$ $\phi = 10.3\%$	20	4.62	2.43	1.90	0.31	0.34	0.15
	40	4.65	2.48	1.88	0.30	0.34	0.15
	60	4.68	2.52	1.86	0.30	0.34	0.16
	80	4.69	2.55	1.84	0.29	0.33	0.16
	100	4.70	2.57	1.83	0.29	0.33	0.17
	200	4.73	2.63	1.80	0.28	0.33	0.17
	400	4.81	2.70	1.78	0.27	0.34	0.18
529.6 m $\rho = 2.51 \text{ g cm}^{-3}$ $\phi = 10.5\%$	20	4.45	2.35	1.90	0.31	0.31	0.14
	40	4.49	2.43	1.85	0.29	0.31	0.15
	60	4.52	2.48	1.82	0.29	0.31	0.15
	80	4.58	2.51	1.82	0.29	0.32	0.16
	100	4.56	2.54	1.80	0.28	0.31	0.16
	200	4.64	2.63	1.76	0.26	0.31	0.17
	400	4.77	2.70	1.77	0.26	0.33	0.18
569.40 m $\rho = 2.55 \text{ g cm}^{-3}$ $\phi = 8.9\%$	20	4.65	2.25	2.07	0.35	0.38	0.13
	40	4.74	2.31	2.05	0.34	0.39	0.14
	60	4.71	2.36	2.00	0.33	0.38	0.14
	80	4.73	2.40	1.97	0.33	0.37	0.15
	100	4.74	2.43	1.95	0.32	0.37	0.15
	200	4.80	2.51	1.91	0.31	0.37	0.16
	400	4.92	2.58	1.91	0.31	0.39	0.17
624.4 m $\rho = 2.67 \text{ g cm}^{-3}$ $\phi = 5.1\%$	20	4.93	2.54	1.94	0.32	0.42	0.17
	40	5.02	2.60	1.93	0.32	0.43	0.18
	60	5.07	2.66	1.91	0.31	0.43	0.19
	80	5.10	2.70	1.89	0.30	0.43	0.19
	100	5.13	2.80	1.83	0.29	0.42	0.21
	200	5.20	2.85	1.82	0.28	0.43	0.22
	400	5.29	2.91	1.82	0.28	0.45	0.23
672.4 m $\rho = 2.71 \text{ g cm}^{-3}$ $\phi = 1.4\%$	20	5.53	3.11	1.78	0.27	0.48	0.26
	40	5.59	3.13	1.78	0.27	0.49	0.27
	60	5.63	3.16	1.78	0.27	0.50	0.27
	80	5.65	3.17	1.78	0.27	0.50	0.27
	100	5.67	3.18	1.78	0.27	0.51	0.27
	200	5.72	3.21	1.78	0.27	0.52	0.28
	400	5.78	3.23	1.79	0.27	0.53	0.28

TABLE 3. Regression Line Parameters

Equation	Slope	Intercept	r
$V_p = mz + b$ (km)	2.1 1/s	3.7 km/s	0.80
$V_s = mz + b$ (km)	0.9 1/s	2.1 km/s	0.64
$V_p = m\rho + b$ (g/cm ³)	4.5 $\frac{\text{km/s}}{\text{g/cm}^3}$	-6.9 km/s	0.91
$V_s = m\rho + b$ (g/cm ³)	2.4 $\frac{\text{km/s}}{\text{g/cm}^3}$	-3.5 km/s	0.88
$V_p = m\phi + b$ (%)	-0.096 km/s	5.3 km/s	-0.86
$V_s = m\phi + b$ (%)	-0.051 km/s	2.9 km/s	-0.84

z: depth, ρ : density, ϕ : porosity, r: correlation coefficient

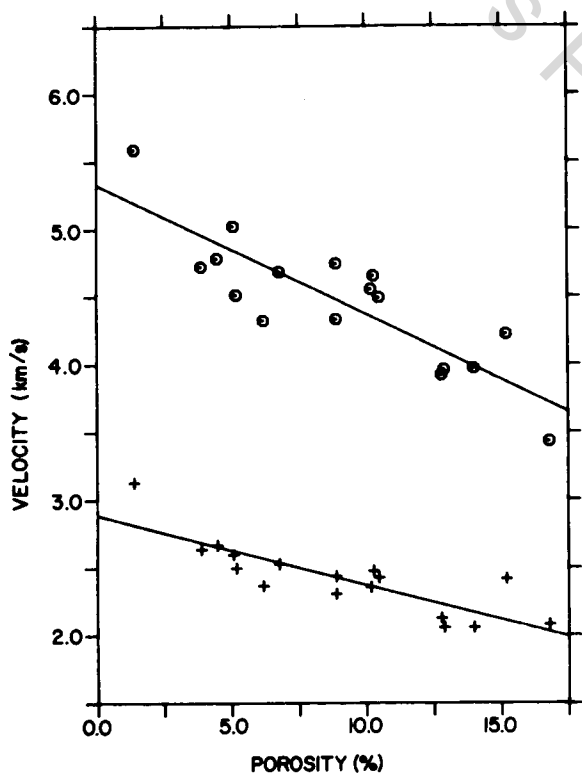


Figure 3: Compressional (0) and shear (+) wave velocities versus porosity at 40 MPa confining pressure.

Low seismic velocities in the upper portion of Layer 2 are commonly attributed to the presence of fractures (Hyndman and Drury, 1976). As was discussed earlier, strong support for this explanation is found in many oceanic regions where laboratory measurements of DSDP cores give significantly higher velocities than those determined by refraction and borehole techniques. In Hole 504B, for example, where sample velocities range narrowly between 5.7 and 6.3 km/s, the compressional wave formation velocities measured both by logging (Salisbury et al., 1985) and by refraction (Stephen and Harding, 1983) increase steadily from 4.0 to 6.0 km/s in response to crack closure in the uppermost kilometre of the volcanics. While the velocity gradient measured in samples from Hole CY-2a is nearly identical to that in Hole 504B, our measurements in the Cyprus volcanics suggest that such gradients may also originate from changes in mineralogy and microporosity. Thus, the positive velocity gradient within Layer 2 may locally originate from decreasing microporosity and increasing metamorphic grade with depth rather than decreasing cracks and fractures.

ACKNOWLEDGEMENTS

This study was supported by NSF Grant No. 8311776AZ, ONR contract N00014-84-K-0207, and NSERC Grant No. IRP-8403.

REFERENCES

- Bednarz, U., Sunkel, G. and Schmincke, H.-U.
 1987: The basaltic andesite-andesite and the andesite-dacite series from ICRDG drill holes CY-2 and CY-2a. I. Lithology, petrology and geochemistry; *in* Cyprus Crustal Study Project Initial Report Hole CY2-2a, ed. P.T. Robinson, I.L. Gibson and A. Panayiotou; Geological Survey of Canada, Paper 85-29.
- Birch, F.
 1960: The velocity of compressional waves in rocks to 10 kilobars, Part 1; *Journal of Geophysical Research*, v. 65, no. 4, p. 1083-1102.
- Christensen, N.I.
 1985: Measurements of dynamic properties of rock at elevated temperatures and pressures; *in* Measurement of Rock Properties at Elevated Pressures and Temperatures, American Society for Testing and Materials, Special Technical Publication 869, ed. H.J. Pincus and E.R. Hoskins; American Society for Testing and Materials, Philadelphia, no. 869, p. 93-107.
- Christensen, N.I. and Salisbury, M.H.
 1975: Structure and constitution of the lower oceanic crust; *Reviews of Geophysics and Space Physics*, v. 13, no. 1, p. 57-86.
- Christensen, N.I. and Smewing, J.D.
 1981: Geology and seismic structure of the northern section of the Oman ophiolite; *Journal of Geophysical Research*, v. 86, no. B4, p. 2545-2555.
- Helmberger, D.V. and Morris, G.B.
 1969: A travel time and amplitude interpretation of a marine refraction profile: primary waves; *Journal of Geophysical Research*, v. 74, no. 2, p. 483-494.
- Houtz, R. and Ewing, J.
 1976: Upper crustal structure as a function of plate age; *Journal of Geophysical Research*, v. 81, no. 14, p. 2490-2498.
- Hyndman, R.D. and Drury, M.J.
 1976: The physical properties of oceanic basement rocks from deep drilling on the Mid-Atlantic Ridge; *Journal of Geophysical Research*, v. 81, no. 23, p. 4042-4052.
- Raitt, R.W.
 1963: The crustal rocks; *in* The Sea, Ideas and Observations on Progress in the Study of the Seas, Volume 3, The Earth beneath the Sea, ed. M.N. Hill; John Wiley and Sons, New York, v. 3, p. 85-102.
- Robinson, P.T. and Gibson, I.L.
 1983: Cyprus Crustal Study Project. Hole CY-2a Lithologic Unit Summaries.
- Salisbury, M.H. and Christensen, N.I.
 1978: The seismic velocity structure of a traverse through the Bay of Islands ophiolite complex, Newfoundland: an exposure of oceanic crust and upper mantle; *Journal of Geophysical Research*, v. 83, no. B2, p. 805-817.
- Salisbury, M.H., Christensen, N.I., Becker, K. and Moos, D.
 1985: The velocity structure of Layer 2 at Deep Sea Drilling Project Site 504 from logging and laboratory experiments; *in* Initial Reports of the Deep Sea Drilling Project, Volume 83, ed. R.N. Anderson, J. Honnorez, K. Becker, et al.; U.S. Government Printing Office, Washington, D.C., v. 83, p. 529-539.
- Stephen, R.A. and Harding, A.J.
 1983: Travel time analysis of borehole seismic data; *Journal of Geophysical Research*, v. 88, no. B10, p. 8289-8298.